Expansion on the loess gully sidewall: Processes and mechanisms

Yulei Ma[1], Xiangzhou Xu[*1], Peiqing Xiao[2], Qiao Yan[1], Chao Zhao[1]
1 Institute of water environment, Dalian University of Technology, Dalian 116024, China
2 Key Laboratory of Process and Control of Soil Loss on the Loess Plateau, Yellow River Institute of Hydraulic Research, Zhengzhou 450003, China
*Corresponding Author, e-mail: xzxu@dlut.edu.cn

Abstract

Gully sidewall expansion is an important geomorphic natural hazard, and the expansion destroys a large extent of agricultural land in the loess regions every year. The main aim of this study was to identify the mechanisms behind gully sidewall expansion through a series of simulated rainfall experiments. The results show that land loss on the gentle slope was the result caused by the water and gravity erosions, and gravity erosion was the primary driving force. The correlation coefficient between the area of land loss on gentle slope and volume of gravity erosion on the gully sidewall was 0.93, and the correlation coefficient between the area of land loss on gentle slope and volume of water erosion was 0.71. The gravity erosion was the dominant impetus driving the change in slope gradient of the gully sidewall. The amount of gravity erosion in 17 of the 19 rainfall events causing a change greater than 5° in the slope gradient of the gully sidewall accounted for more than 50% of the total amount of sidewall erosion. Furthermore, the dynamic variation of the retreat rates for the gully shoulder line showed a similar trend to that of the total volume of sidewall erosion, and exhibited an increase-decrease-increase tendency. The most significant factors affecting the change in slope gradient of the gully sidewall and retreat rate of the gully shoulder line were the rainfall duration and intensity, of which the sensitivity coefficients were 2.2 and 4.0, respectively. As a result, a combination of vegetation measures on the gentle slope, structural and ecological practices on the sidewall, and powerful structural practices, e.g., check dams, on the gully floor, is preferred for sidewalls vulnerable to expansion.

Keywords: Sidewall expansion, Gravity erosion, Water erosion, Rainfall, Landform

1 Introduction

Gully sidewall expansion, particularly in loess terrains, represents an undeniable reality both as a geomorphic process and as a type of hazard. Gully sidewall expansion—also known as gully sideward extension (Veness, 1980), gully sidewall erosion (Blong et al., 1982) and gully bank retreat (Chaplot et al., 2011)—is attributed to the combined effects of gravity erosion (landslides, avalanches and mudslides) and water erosion (by splash and runoff) (Chaplot et al., 2011). As a result of these processes, the sidewall retreats towards the gentle slope, releasing sediment to the gully, decreasing the cultivated area around the gully, and exposing new gully walls to erosion, eventually threatening local ecology and food security (Wijdenes and Bryan, 2001; Spalevic et al., 2013). According to some estimates, sidewall expansion can amount to more than 50% of the total sediment produced in gullies (Martínez-Casasnovas et al., 2004). Most studies have primarily focused on the expansion rate of the gully sidewall using remote-sensing images (Yan et al., 2014), and protection measures to mitigate gully sidewall expansion (Wang et al., 2019). Wang et al. (2019) suggested that the effectiveness of existing protection measures to control gully bank retreat was clear only in the short-term, while their long-term effectiveness remains unclear. Understanding the processes and mechanisms of gully sidewall erosion is important for implementing effective measures to reduce expansion. However, few studies have specifically addressed the processes, mechanisms and controls of gully sidewall expansion.

Gully sidewall expansion is influenced and constrained by many factors, such as slope material, topography and rainfall (Ali et al., 2014; Xu et al., 2015). Chaplot et al. (2011) indicated that raindrop runoff and splash could directly remove soil from the gully sidewall. Rainfall also indirectly causes sidewall instability by increasing the sidewall weight due to the addition of moisture (Lomtadze, 1977). The slope height and gradient are important geometric parameters of the gully sidewall. An increase in the slope height or gradient will cause stress to concentrate in a zone on the slope, resulting in soil mass displacement down from the escarpment (Lu and God, 2013). In addition, the downslope component of gravity increases as the slope gradient increases, thus reducing gully sidewall stability. Consequently, the processes and mechanisms of sidewall expansion under the influence of multiple factors are complicated.

Gully sidewall extension is an important process in gully development (Blong et al., 1982), and its dynamic nature can be assessed from changes in the gully shoulder line (Liu et al., 2016). The gully shoulder line is the line that intersects the gentle slope and gully sidewall (Fig. 2), also called the edge-line of gentle slope (Chen and Cai 2006) or line of gully boundary (Wu et al., 2008). The gully shoulder line is one of the most important landform demarcations for geomorphic analysis and land-use planning on the Loess Plateau (Yan et al., 2014). The existing research has focused on the methodology extracting the gully shoulder line, and relatively few studies have examined

the factors influencing the retreat of the gully shoulder line (Qin et al., 2010; Yan et al., 2014). Thus, in this study, the direct effects of topography and rainfall on the retreat rate of the gully shoulder line were examined.

The extent of change in the slope gradient on the gully sidewall can also mirror the intensity of the sidewall expansion and the stage of gully development. The slope gradient influences the scale and intensity of material flow and energy conversion at the earth's surface (Tang et al., 2003). For instance, the infiltration, runoff and flow energy of a slope are significantly affected by the slope gradient (Assouline and Ben-Hur, 2006; Zheng and Xiao 2010). Consequently, the slope gradient directly restricts the landform morphology, runoff development and soil erosion, and also influences, to a relatively great or little extent, the evolution of natural soil and change in the land quality (Wang et al., 2005). A change in slope gradient influences the degree of the erosion of soil and migration of surface materials, and can also be interpreted as the result of space redistribution among the gully sidewall, channel floor and gentle slope. Defined development periods indicate stage-specific features for the slope gradient (Wang et al., 2005). Hence, by exploring the changing characteristics of the slope gradient on gully sidewalls and identifying the dominant mechanisms for dynamic change in sidewall slopes.

Understanding of gully sidewall expansion should be considered by further in-situ and modeling studies (Chaplot, 2013). Gravity erosion is difficult to predict due to its sudden occurrence, such process-based data of gully sidewall expansion are difficult to obtain under natural rainfall conditions. However, a physical model of a selected geomorphological feature, produced under closely controlled conditions, would be an effective way to dynamically observe the process of gully sidewall expansion in much shorter times, to search for the mechanisms behind gully sidewall expansion, and to deeply examine interacting factors and their various influences on expansion processes. Chorley (1964) identified three broad classes of physical models – segments of unscaled reality, scale models, and analog models – with the former being the most widespread in the field of soil and water conservation. In this study, the model slope was made based on field investigations and was a segment of unscaled reality.

The gully sidewall expansion on the Loess Plateau is remarkable because the gully density in the area is very large, of which 270,000 gullies are longer than 500 m (Liu et al., 2013). Loess gully sidewalls, which are gully banks usually with gradients of more than 70° (Fig. 1), are prone to erosion under the action of water and gravity during rainstorms, because the slope material is mostly silty sandy loam with a loose structure, as well as being highly porous and having vertical joints (Xu et al., 2004). Usually, most soil erosion is triggered by short-burst rainfall events, where the rainfall intensity is greater than 0.5 mm min-1 and the rainfall duration ranges from 30 to 120 min (Wang and Jiao 1996; Wang et al., 2016; Jiao et al., 2001).

Sensitivity analysis has been widely utilized in soil erosion studies to reveal the relative importance of impact factors (Sánchez-Canales et al., 2015; Xu et al., 2015a). Gully sidewall expansion is a complicated process that involves a number of interactive factors. When a factor exceeds its critical value, it may become the dominant factor to trigger gully sidewall expansion (Yang et al., 2011). The method of sensitivity analysis can help in identifying the dominant factors of gully sidewall expansion, including the geology, topography and rainfall. In this study, the sensitivity of the developing features of gully sidewall expansion (i.e., variations in the slope gradient of the sidewall and retreat rates of the gully shoulder line) on the rainfall and topography have been evaluated based on the increase-rate-analysis method (Xu et al., 2015a).

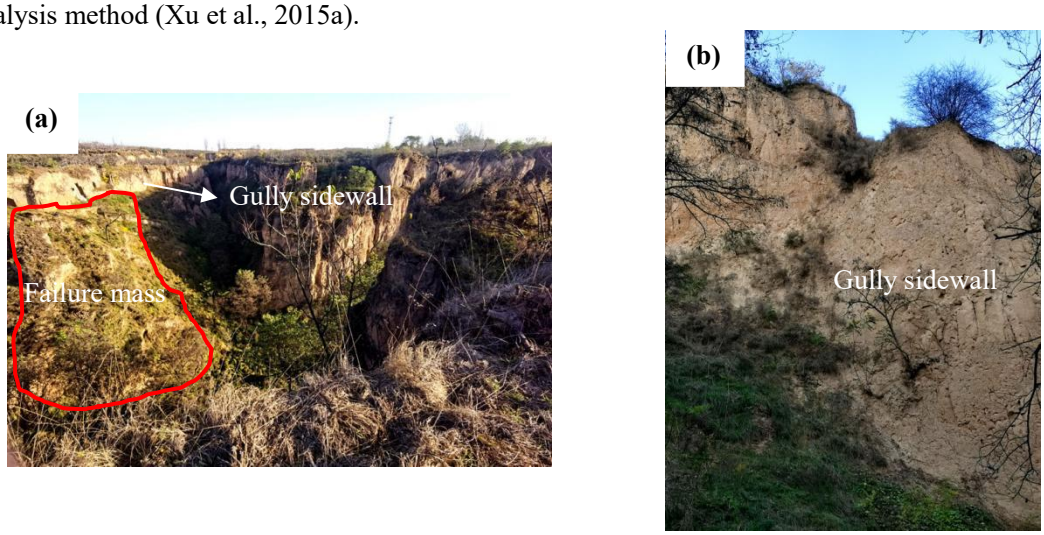

Figure 1 Photographs showing the representative loess gully sidewall on the Loess Plateau of China. (a) Gravity erosion on the gully sidewall, and (b) a typical gully sidewall with a slope gradient of more than 700.

Using a series of simulated rainfall experiments, this study aimed to understand the principal causes and mechanisms of gully sidewall expansion. The impact of gravity erosion on gully sidewall expansion was quantified,

and the characteristics of gully sidewall expansion under the actions of gravity and water erosions were explored.

2 Materials and methods

A series of gully sidewall expansion experiments were conducted in 2010 and 2012 in the Joint Laboratory for Soil Erosion at the Dalian University of Technology and Tsinghua University, located in Beijing, China. Although the experiments have been completed by the corresponding author and his team for years, no similar experiments have been found by the authors in the references up to the present. The landscape simulator included a rainfall simulator, a conceptual landform and a topography meter (Fig. 2). The geometry of the conceptual landform was designed based on field investigations on the Loess Plateau. The conceptual landforms were 3 m long, 3 m wide and 1 or 1.5 m high, with a gentle slope (above the gully shoulder line) of 3° and a gully sidewall slope (below the gully shoulder line) of 70 or 80°. The test soil had a median particle diameter of 0.05 mm and a specific gravity of 2.56. Before starting each rainfall event experiment, a small intensity of rainfall was applied to the landform, and the experiment would start soon after the surface soil began to runoff generation. An SX2009 sprayer-typed rainfall simulator, designed by the authors, was used to simulate the rainfalls in the experiments. The rainfall intensities were 0.8 and 2.0 mm min^{-1}, with rainfall durations of 30 and 60 min in the experiments.

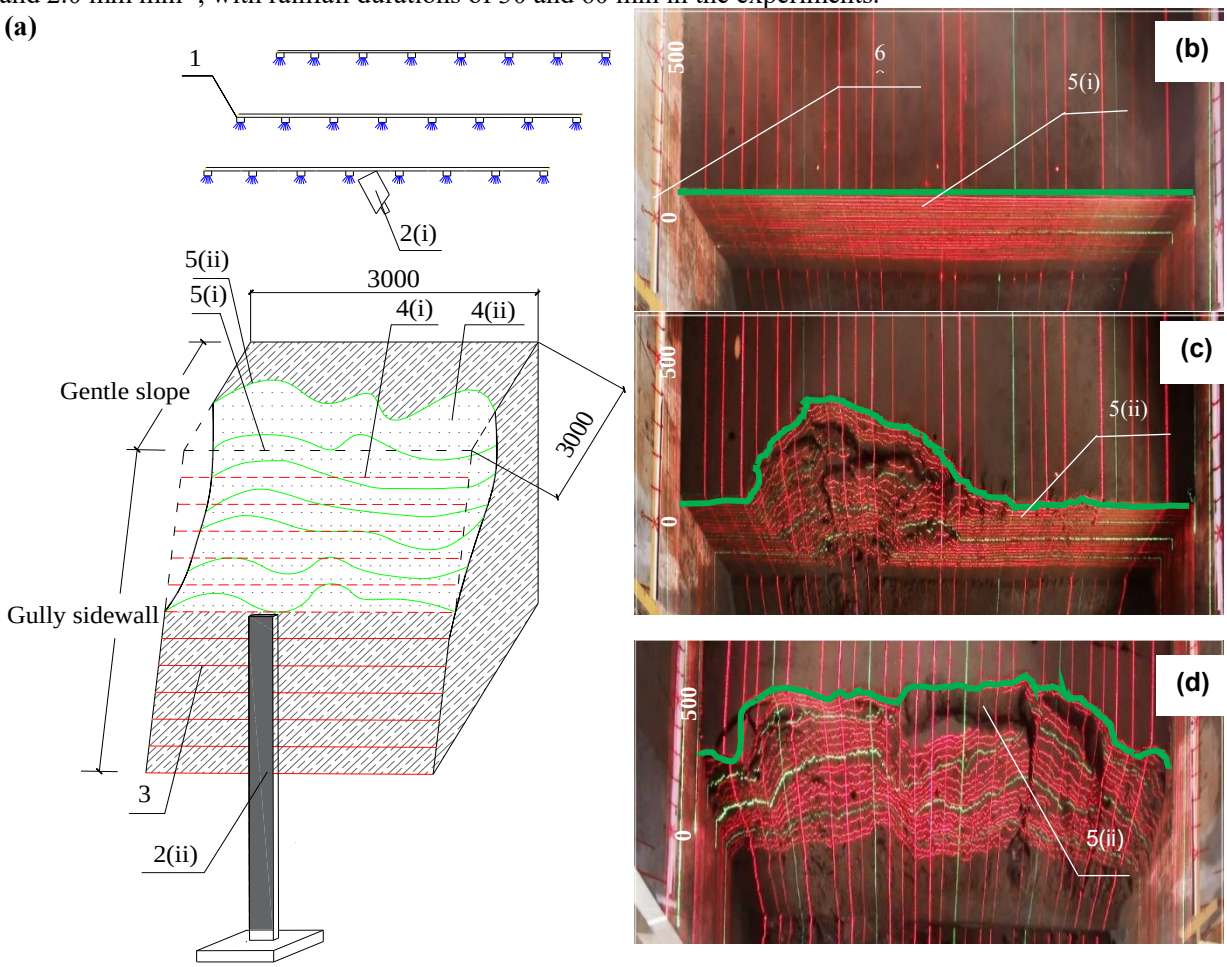

Figure 2 Landscape simulator in which the rainfall simulation experiments were conducted. All units in mm. (a) Schematic of the topography meter measurement system. (b) An image of the initial gully sidewall in experiment L6. (c, d) Images of sidewall retreat after the first and third rainfall events in experiment L6. *1* – rainfall simulator, *2* – topography meter (*i* – camera with collimator, *ii* – laser source), *3* – equidistant horizontal projections, *4* – model slope (*i* – initial model slope, *ii* – model slope after sidewall expansion), *5* – gully shoulder line (*i* – original gully shoulder line, *ii* – gully shoulder line after sidewall expansion), and *6* – positioning marks

The uniformity coefficients of the simulated rainfall exceeded 80%. Each conceptual landform was subjected to five runs of rainfall, with the interval being approximately 12 h. The experimental setup is listed in Table 1. The MX-2010-G topography meter included a set of laser sources and a camera with a collimator (Fig. 2), and was applied to observe the process of sidewall expansion under the simulated rainfalls. The occurrence time and location of gravity

erosion and the behavior of the sidewall expansion were recorded using a video camera. A set of parallel laser lines, equivalent to contour lines, were emitted from the topography meter to the sidewall surface, which helped to transform the target-plane figures into 3D graphs (Fig. 3). As shown in Fig. 3, after a comparison of the images of the gully sidewall, pre- and post-failure, we obtained the erosion data, including the areas of land loss on the gentle slope, the volumes of gravity erosion and total soil erosion, the retreat rates of the gully shoulder line, and the slope gradients of the sidewalls. The relative error in the volumes recorded with the MX-2010-G topography meter was less than 10% (Xu et al., 2015b).

The volume of soil erosion was calculated as follows:

$$W_{Vj} = T_{Vj} - G_{Vj} \quad (1)$$

where j is the sequence number of the rainfall event in an experiment with j = 1, 2, …, 5; W_{Vj} is the volume of water erosion in the j^{th} rainfall (cm^3); G_{Vj}, is the total volume of gravity erosion, which is the sum of the volumes of all the gravity erosion events occurring during the j^{th} rainfall in an experiment (cm^3); T_{Vj}, is the total volume of sidewall erosion, which is equal to the difference between the slope volume before and after the j^{th} rainfall in an experiment (cm^3).

The steps for extracting the area of land loss on the gentle slope were as follows. First, the picture was loaded with the control points in the software R2V, the gully shoulder line was portrayed, and then the two control points were connected below the gully shoulder line as a fixed baseline. Second, the above file was output with the format *.dxf. respectively. Third, this vector file (*.dxf) was imported into AutoCAD, vertical lines were drawn from the shoulder line to the baseline, a closed curve was formed, and then the area was calculated. Then, the total area of land endpoints of the gully loss on the gentle slope, A_R, was obtained as follow:

Table 1 Rainfall and topography conditions for experiments L1–L10. Three rainfalls, two initial slope gradients and two slope heights of the gully sidewall were considered in the experiments.

Test umber	Sidewall configuration		Rainfall		
	Height (m)	Gradient (°)	Intensity (mm min^{-1})	Duration (min)	Runs
L1	1.0	70	2.0	30	5
L2	1.0	80	2.0	30	5
L3	1.5	70	2.0	30	5
L4	1.5	80	2.0	30	5
L5	1.0	70	0.8	60	5
L6	1.0	80	0.8	60	5
L7	1.5	70	0.8	60	5
L8	1.5	80	0.8	60	5
L9	1.0	70	0.8	30	5
L10	1.0	80	0.8	30	5

$$A_R = \sum_{j=1}^{N} A_{Rj} \quad (2)$$

where A_R is the total area of land loss on the gentle slope after five rainfall events in an experiment (cm^2); A_{Rj} is the area of land loss on the gentle slope between the gully sidewall shoulder line before and after the j^{th} rainfall in an experiment (cm^2); and N is the number of rainfall events in an experiment.

The retreat rate of the gully shoulder line, V_R, can be calculated using the following formula:

$$V_R = \sum_{j=1}^{N} \frac{A_{Rj}}{Lt} \Big/ 5 = \sum_{j=1}^{N} V_{Rj} \Big/ 5 \quad (3)$$

where V_R is the average retreat rate of gully shoulder line during five rainfall events in an experiment (cm min^{-1}); V_{Rj} is the retreat rate of the gully shoulder line during the j^{th} rainfall in an experiment (cm min^{-1}); t is the rainfall duration (min); and L is the linear distance between the two endpoints of the original gully shoulder line (cm).

Only was the slope gradient of the gully sidewall discussed in the paper because hardly any erosion occurred on the gentle slope with the gradient of 3°, and all of the gravity erosions and most of the water erosions happened on

the sidewall. The slope gradient of the gully sidewall was measured using the following steps. First, the block ArcScene was opened in the software ArcGIS10.6, the 3D surface models—triangulated irregular networks (TINs)—were imported and transformed into raster formats, then the slope gradients of the 3D TINs were obtained using the command *Slope* under *Raster Surface*. Second, the 3D TINs were converted into vector files using the command *Surface Slope* under *Triangulated Surface*, and the vector files corresponding to the gully sidewall were obtained by the command *Delete* under *3D Editor*. Third, the slope gradient of the gully sidewall was calculated using the vector data obtained in step 2 as clip features to clip the raster data obtained in step 1. Then, the difference in slope gradient of the gully sidewall, D_g, was obtained as follow:

$$D_g = \sum_{j=1}^{N} D_{gj} = \sum_{j=1}^{N} D_{gb} - D_{ga} \quad (4)$$

where D_g is the difference between the slope gradient of the gully sidewall before the first rainfall and that after the fifth rainfall in an experiment (°); D_{gj} is the difference in the slope gradient of gully sidewall during the j^{th} rainfall (°); and D_{gb} and D_{ga} are the slope gradient of gully sidewall before and after the j^{th} rainfall (°).

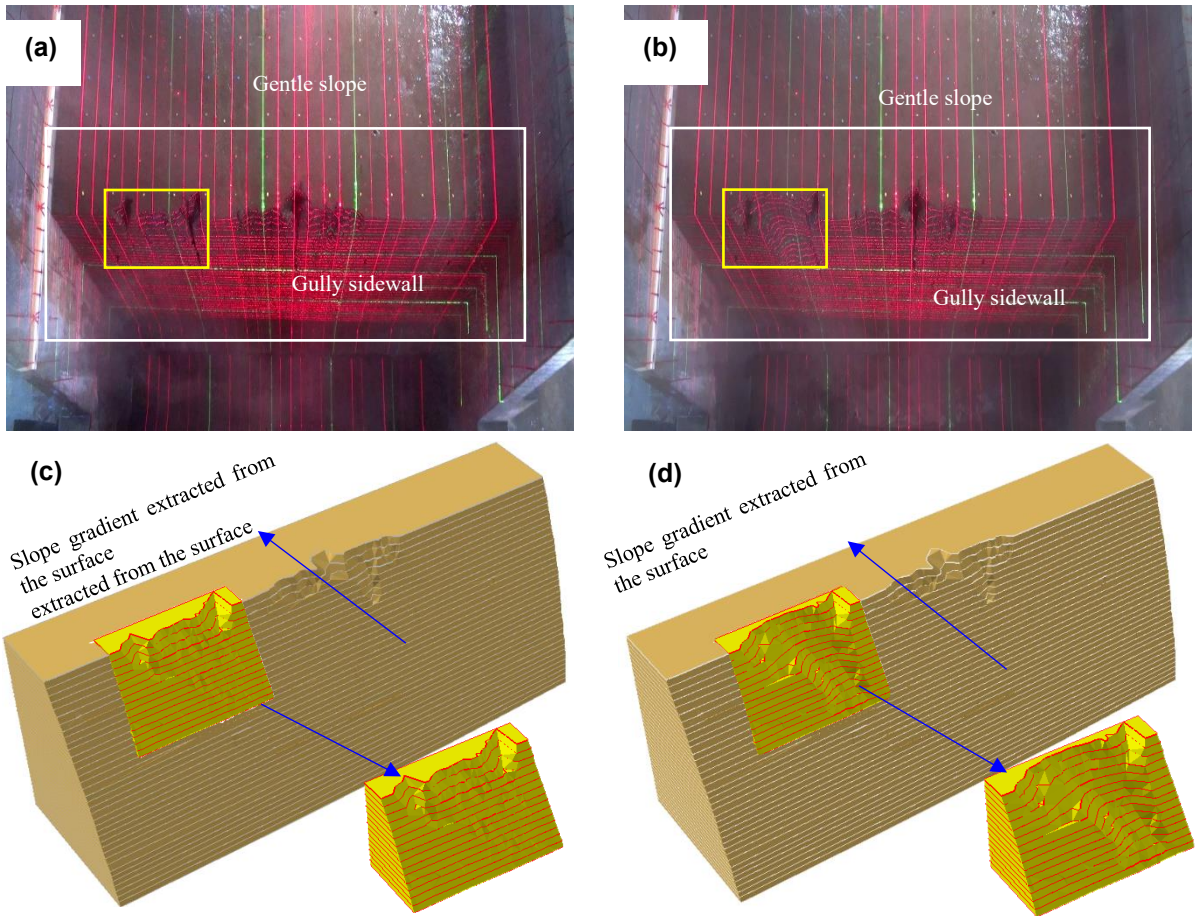

Figure 3 Comparison of the real slopes and 3D images. (a) A photo of the gully sidewall before the start of mass failure, (b) an image of the gully sidewall after a mass failure, and (c) and (d) 3D surface images corresponding to (a) and (b). The differences in the volume and gradient of the gully sidewall in the white frame have been calculated with an individual event of gravity erosion shown in the small yellow frame. The difference in volume and slope gradient of the two sidewalls shown in (c) and (d) are the total amount of soil loss and the average change in slope gradient during a rainfall event, respectively

A sensitivity coefficient, which represents the extent of change in a target value triggered by variation in a crucial factor while keeping other conditions fixed, is the ratio of the percentage change in the target value to the percentage change in the parameter (Xu et al., 2020). A relatively large sensitivity coefficient indicates that the target value is highly susceptible to changes in the influencing factor. To assess the influence of the rainfall and topography factors on D_g and V_R, we divided 10 sets of experiments into the following seven experimental groups: Ga (experiments L1, L2, L5 and L6) vs Gb (experiments L3, L4, L7 and L8), with the slope height in Ga being 1.0 m, and in Gb being

1.5 m; Gc (experiments L1, L3, L5 and L7) vs Gd (experiments L2, L4, L6 and L8), with the initial slope gradients being 70 and 80°, respectively; Ge (experiments L5 and L6) vs Gf (experiments L9 and L10), with the rainfall duration in Gc being 30 min, and in Ge being 60 min; and Gf (experiments L9 and L10) vs Gg (experiments L1 and L2), with the rainfall intensity being 0.8 and 2.0 mm min^{-1}, respectively. The average values of D_g and V_R were calculated for each experimental group ($\overline{D_g}$ and $\overline{V_R}$, respectively). We then employed the increase-rate-analysis method (Xu et al., 2015a) to evaluate the sensitivity of $\overline{D_g}$ and $\overline{V_R}$ to rainfall and topography. The sensitivity coefficients were calculated as follows:

$$S = \frac{R_t}{R_i} = \frac{(T_a - T_b)/T_b}{(I_a - I_b)/I_b} \quad (5)$$

where S is the sensitivity coefficient for assessing the susceptibility of $\overline{D_g}$ or $\overline{V_R}$ to the influencing factors; R_t is the increased ratio of $\overline{D_g}$ or $\overline{V_R}$; R_i is the increased ratio of the influencing factor; T_a represents $\overline{D_g}$ or $\overline{V_R}$ after the influencing factor was changed in an experiment group (° or cm min^{-1}); T_b represents $\overline{D_g}$ or $\overline{V_R}$ before the influencing factor was changed in an experiment group (° or cm min^{-1}); I is one of the influencing factors—initial slope gradient and height, and rainfall duration and intensity; and I_a and I_b represent the values of the influencing factors, after and before the change in an experimental group, respectively.

3 Results

3.1 Variations in the slope gradient of a gully sidewall

Changes in the slope gradients of the gully sidewalls were obvious in the experiments. Table 2 shows these changes during the five rainfall events in experiments L1–L10. After five rainfall events, the slope gradients of the gully sidewalls in experiments L1–L10 were 56.4, 54.5, 45.3, 53.3, 35.0, 37.5, 44.3, 55.6, 61.9 and 63.9°, respectively. Compared to the initial slope gradient in experiments L1–L10, the slope gradients were decreased by 13.6, 25.5, 24.7, 26.7, 35.0, 42.5, 25.7, 24.4, 8.1 and 16.1°, respectively. This implies that the landforms in experiments L5 and L6 tended to stabilize after five rainfall events, probably because the slope gradients were close to the angles of repose of dry and wet loess soil (Meng, 1996).

Table 2 Changes in the slope gradient of the gully sidewall after five rainfall events in experiments L1–L10. Compared with the initial slope gradient in experiments L1–L10, the slope gradients were decreased by an average of 24.2°.

Test number	Slope gradient of the gully sidewall (°)		D_g (°)	Test number	Slope gradient of the gully sidewall (°)		D_g (°)
	Initial	After five rainfalls			Initial	After five rainfalls	
L1	70	56.4	13.6	L6	80	37.5	42.5
L2	80	54.5	25.5	L7	70	44.3	25.7
L3	70	45.3	24.7	L8	80	55.6	24.4
L4	80	53.3	26.7	L9	70	61.9	8.1
L5	70	35.0	35.0	L10	80	63.9	16.1

Notes: D_g, namely the difference in slope gradient of the gully sidewall, means the difference between the slope gradient of the gully sidewall before the first rainfall and that after the fifth rainfall in an experiment.

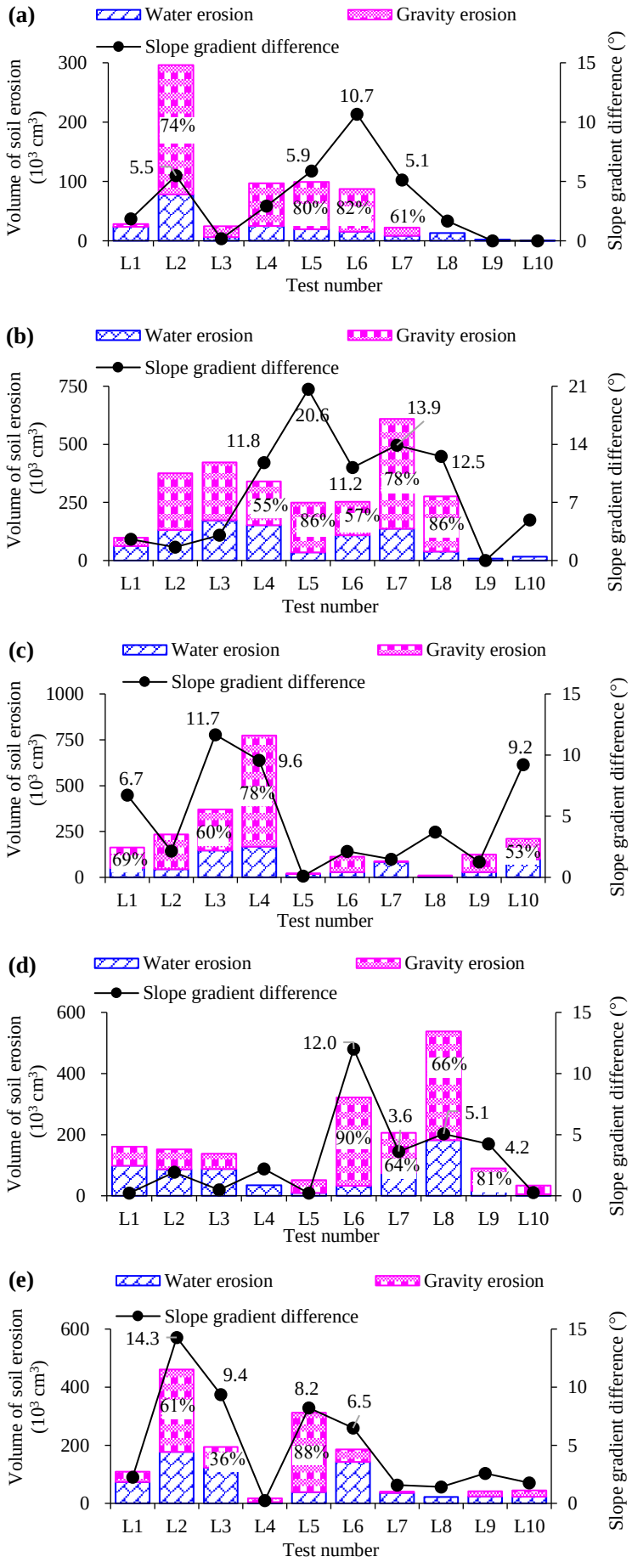

Figure 4 Dynamic changes in the slope gradient of the gully sidewall in response to the volume of gravity and water erosion of a landform during five rainfall events. (a) First rainfall event, (b) second rainfall event, (c) third rainfall event, (d) fourth rainfall event, and (e) fifth rainfall event. The initial slope gradient of experiments L1, L3, L5, L7 and L9 was 70°, while the initial slope gradient of experiments L2, L4, L6, L8 and L10 was 80°

For instance, in the fourth rainfall event of experiments L1–L4, the values of changes in slope gradient of gully sidewall were 0.2, 1.9, 0.5 and 2.2°, respectively, and the corresponding volumes of water erosion accounted for 61, 57, 64 and 100% of the total volume of sidewall erosion, respectively (Fig. 4d). In addition, the volumes of water erosion in the fifth rainfall event of experiments L2 and L6 were comparable, whereas the volumes of gravity erosion in experiment L2 was 11.5 times greater than that in experiment L6, and the slope gradient of gully sidewall in experiment L2 (14.6°) decreased more significant than that in experiment L6 (6.5°) (Fig. 4e).

Gravity erosion was the primary driver influencing the change in slope gradient of the gully sidewall in the experiments. Fig. 4 illustrates the difference in the slope gradient of the gully sidewall during the five rainfall events under the actions of gravity and water erosions. The amount of gravity erosion in 17 of the 19 rainfall events causing a change greater than 5° in the slope gradient of the gully sidewall accounted for more than 50% of the total amount of sidewall erosion. For example, in the second rainfall event of experiments L4–L8, the slope gradient of the gully sidewall decreased by 11.8, 20.6, 11.2, 13.9 and 12.5°, respectively, and the corresponding volumes of gravity erosion accounted for 55, 86, 57, 78 and 86% of the total volumes of sidewall erosion, respectively (Fig. 4b). As shown in Fig. 4c, the volumes of gravity erosion accounted for 69, 60 and 78% of the total volumes of sidewall erosion during the third rainfalls of the experiments L1, L3 and L4, and their slope gradients of the gully sidewalls were reduced by 6.7, 11.7 and 9.6°, respectively. However, when the volume of water erosion during a rainfall event accounted for a large proportion of the total volume of soil erosion, the slope gradients of the gully sidewalls varied only marginally.

3.2 Retreat rate of the gully shoulder line

The gully shoulder line is always located in the most active part of a gully and its dynamics reflect the development of the gully (Liu et al. 2016). The retreat rate of the gully shoulder line mirrors not only the outward appearance of the developing gully, but also the internal mechanisms of gully development (Zhang et al. 2012). As can be seen from the experimental images (Fig. 2b–d), a retreat in the gully shoulder line was evident. Fig. 5 also illustrates the dynamic retreat of the gully shoulder line for the five rainfall events in experiment L8. After the fifth rainfall event, the maximum and minimum retreat widths of the gully shoulder line exceeded 100 and 50 cm, respectively. As shown in Fig.6, the retreat rate of the gully shoulder line and the total volume of soil erosion showed similar variations in experiments L1–L10. Additionally, the total volumes of gravity erosion in experiments L3, L6, L7 and L8 were comparable (approximately 600×10^3 cm^3), whereas their total volumes of water erosion were 538.0, 327.4, 338.6 and 260.9×10^3 cm^3, and their retreat rates of the gully shoulder line were 0.6, 0.4, 0.3 and 0.2 cm min^{-1}, respectively. This implies that the retreat rate of the gully shoulder line is related to the volume of water erosion.

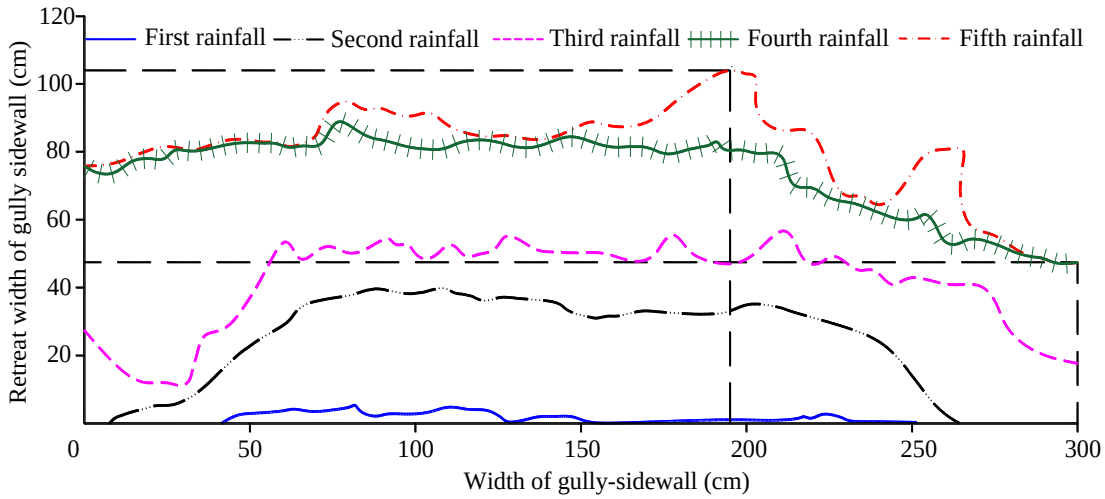

Figure 5 Dynamic changes in the gully shoulder line during five rainfall events in experiment L8. After the fifth rainfall event, the maximum retreat width of the gully shoulder line was more than 100 cm, with the minimum retreat width being more than 50 cm

The retreat rate of the gully shoulder line showed an increasing-decreasing-increasing trend during the five rainfall events in the experiments. For example, as shown in Fig. 7a, in experiment L1, the retreat rate of the gully shoulder line reached a peak value of 0.9 cm min^{-1} in the second rainfall event and reached a minimum value of 0.1 cm min^{-1} in the fifth rainfall event. The retreat rate of the gully shoulder line in experiment L2 reached the peak

values in the second ($V_{R2} = 1.1$ cm min^{-1}) and fifth ($V_{R5} = 2.2$ cm min^{-1}) rainfall events, and a minimum value in the third ($V_{R3} = 0.3$ cm min^{-1}). As shown in Fig. 7b, the retreat rate of the gully shoulder line in experiment L7 reached the peak values of 0.6 and 0.7 cm min^{-1} in the second and fourth rainfall events, respectively. Comparing Fig. 7a and b, it can be seen that the retreat rates of the gully shoulder lines in the experimental group with a rainfall intensity of 2.0 mm min^{-1} were significantly greater than in the experimental group with a rainfall intensity of 0.8 mm min^{-1}.

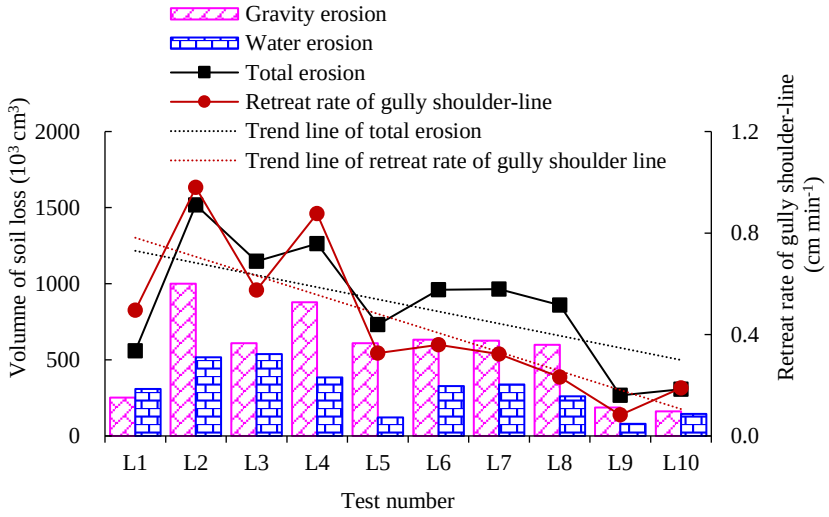

Figure 6 Retreat rate of the gully shoulder line in response to the volume and type of soil erosion after five rainfall events in experiments L1–L10. The total volume of soil erosion was equal to the sum of the volumes of the gravity and water erosion after five rainfall events for each experiment. The retreat rate of the gully shoulder line is the average retreat rate of the gully shoulder line during five rainfall events

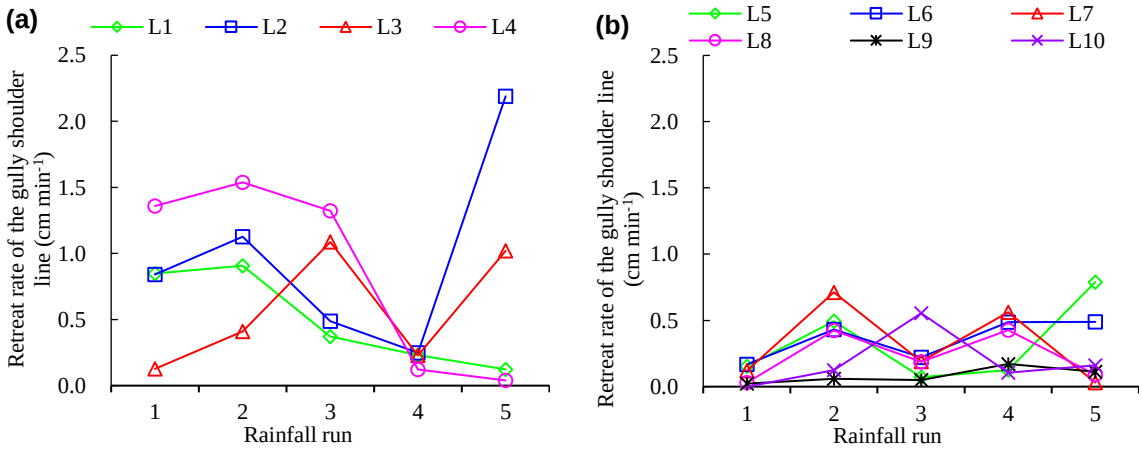

Figure 7 Retreat rate of the gully shoulder line during each rainfall event in experiments L1–L10. (a) Severe rainstorms with a density of 2.0 mm min^{-1}, and (b) gentle rainfall with a density of 0.8 mm min^{-1}

3.3 Land loss on the gentle slope

Different types of erosion may significantly influence the area of land loss on the gentle slope. In this study, we investigated the relationship between the area of land loss on the gentle slope and volumes of different types of soil erosions, namely gravity and water erosions, during the process of sidewall expansion. As shown in Fig. 8, the correlation coefficient between the area of land loss on gentle slope and volume of gravity erosion on the gully sidewall was 0.93, and the correlation coefficient between the area of land loss on gentle slope and volume of water erosion on the gully sidewall was 0.71. This shows that land loss on the gentle slope was the result caused by the water and gravity erosions, and the gravity erosion was the primary driving force. The soil on the gentle slope was separated from the slope face under the effect of gravity, accumulating on the downslope or gully bottom and resulting in an irreversible loss of land.

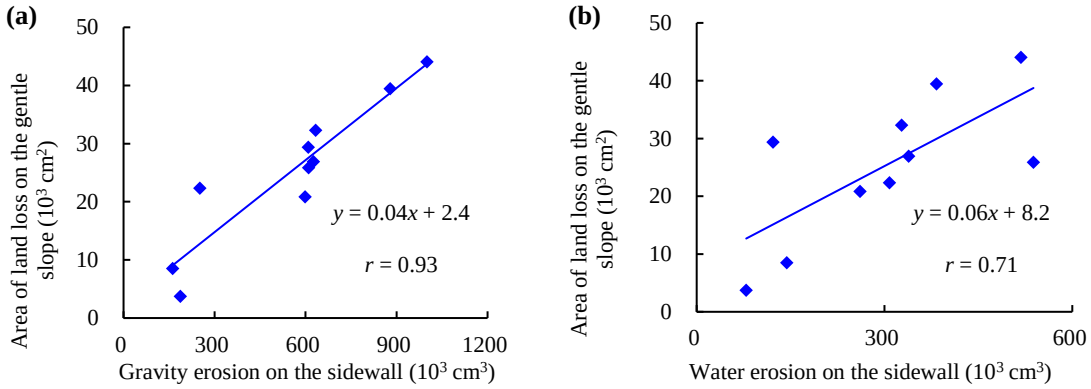

Figure 8 Correlation between the soil erosion on the sidewall and land loss on the gentle slope after five rainfall events in experiments L1–L10. (a) Gravity erosion on the sidewall vs. land loss on the gentle slope, and (b) water erosion on the sidewall vs. land loss on the gentle slope

3.4 Sensitivity coefficients

Rainfall duration and initial slope gradient significantly influenced the changes in slope gradient of the gully sidewalls in the experiments. As shown in Fig. 9, there were substantial increases in the change in slope gradient of the gully sidewall when the rainfall intensity, rainfall duration and initial slope gradient increased. In particular, when the other factors were fixed, but the rainfall duration was increased from 30 to 60 min, the change in slope gradient of the gully sidewall grew from 12.1 to 38.8°. In contrast, the change in slope gradient of the gully sidewall dropped with the increasing slope height. A sensitivity analysis was implemented to assess the influences of topography and rainfall on the change in slope gradient of the gully sidewall. The sensitivity coefficients of the change in slope gradient of the gully sidewall on rainfall duration, initial slope gradient, rainfall intensity and slope height were 2.2, 1.4, 0.4 and -0.3, respectively (Fig. 9). These results indicate that rainfall duration and initial slope gradient were the most and second-most influential factors on the changes in slope gradient of the gully sidewalls in the experiments.

Rainfall intensity and initial slope gradient were the most important sensitivity parameters affecting the retreat rate of the gully shoulder line in the experiments. Fig. 10 illustrates the variation in the retreat rate of the gully shoulder line as rainfall and topography increased. It was found that the retreat rates of the gully shoulder line increased with increasing rainfall intensity, rainfall duration and initial slope gradient. For example, when the other conditions were fixed, but the rainfall intensity was increased from 0.8 to 2.0 mm min^{-1}, the retreat rate of the gully shoulder line increased by 600% (with the retreat rate increasing from 0.1 to 0.7 cm min^{-1}). However, when the slope height increased from 1.0 to 1.5 m, the retreat rate of the gully shoulder line was maintained at approximately 0.5 cm min^{-1}. Using a sensitivity analysis with the increase-rate-analysis method, the authors found that the sensitivity coefficients of the retreat rate of gully shoulder line on rainfall intensity, initial slope gradient, rainfall duration and slope height were 4.0, 3.5, 2.0 and -0.1, respectively (Fig. 10). These results suggest that the most significant factors affecting the retreat rate of gully shoulder line were the rainfall intensity and initial slope gradient.

4 Discussion

4.1 Mechanisms of gully sidewall expansion

The variation in slope gradient of the gully sidewalls was the result of the synergetic effect of water and gravity erosions, although significant decreases in slope gradient were caused by gravitational erosion (Fig. 4). Water erosion occurred first, increasing the occurrence and development of gravity erosion during the process of sidewall expansion. The movement of topsoil towards the downslope position due to runoff was the result of increasing stress and decreasing strength at the soil surface during rainfall. This process changed the topography, such as some parts of the gully slope becoming steep, thus increasing the possibility of mass failure (Lu and Godt, 2013). Conversely, gravity

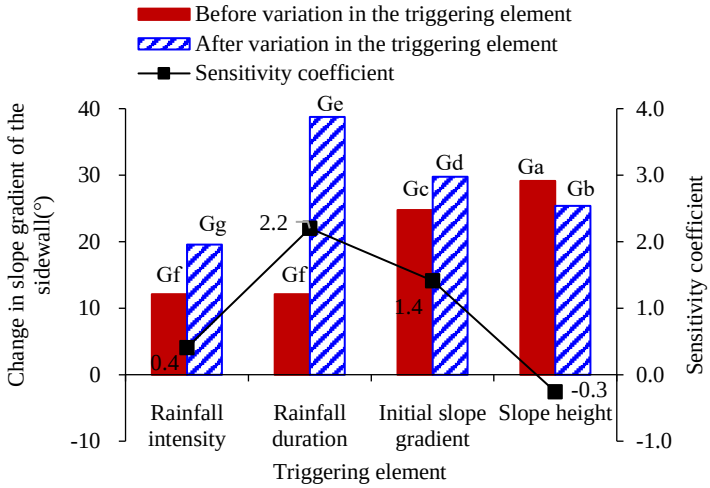

Figure 9 Sensitivity analysis of changes in the slope gradient of the gully sidewall for the triggering elements. The changes in the slope gradients of the gully sidewalls in the experimental groups Ga–Gg ranged from 12.1 to 38.8°

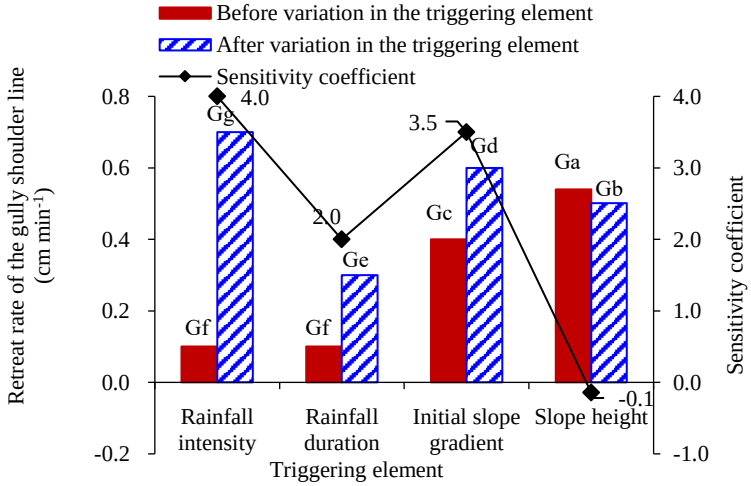

Figure 10 Sensitivity analysis of the retreat rate of the gully shoulder line for the triggering elements. The average retreat rates of the gully shoulder line in experimental groups Ga–Gg ranged from 0.1 to 0.7cm min^{-1}

erosion destroyed the original structure of the soil as the structure became loose, providing a major source of water erosion. In the experiments, the slope gradient of the gully sidewalls was significantly reduced owing to the occurrence of large-scale failure or a large number of small-scale failures that allowed for temporary stability of the gully sidewall. Water erosion then became the main erosion pattern of the gully sidewall, as evidenced with the erosion from the gully sidewall caused by surface runoff and that from the soil accumulation caused by channel flow. Because much of the material produced by the gravity erosion remained at the toe of the gully sidewall, the deposition may have increased the instability of the gully sidewall. Liu and Wu (1993) also suggested that the processes of water and gravity erosions mutually influence each other in the gully development.

The retreat of the gully shoulder line was also influenced by a combination of gravitational and hydraulic erosion. The gully shoulder is a heavily eroded area, characterized with the rapid retreat of the gully shoulder line. In the experiments, soil erosion started from the gully shoulder (Fig. 3a and b). The rapid retreat of the gully shoulder line is likely due to two reasons. First, the formation of runoff provides a driving mechanism for soil erosion (Lu and Godt, 2013). After the formation of infiltration-excess runoff on the loess gentle slope, the runoff flows through the gully shoulder, eroding it, with the intensity of the erosion gradually decreasing from the gully shoulder to the downslope. In addition, with an increase in rainfall duration, the stress distribution in a slope is dynamic, whether caused by water movement or mass gravity. Tensile cracks form at the top of the slope, owing to a decrease in the cohesion and an increase in the downslope component of gravity in the gully sidewall, as the soil water content increases under rainfall infiltration. Pore water pressure is generated after rainwater enters these tension cracks, causing tension crack propagation and coalescence, followed by the formation of a potential slip surface. When the strength at the slip surface decreases with an increase in pore water pressure (Orense, 2004), gravity erosion occurs,

accompanied with retreat of the gully shoulder line.

4.2 Effects of parameters on gully sidewall expansion

Changes in rainfall and topography significantly influence the process of sidewall extension, such as dynamic changes in erosion patterns and slope gradients (Thornes and Alcantara-Ayala, 1998; Sánchez-Canales et al., 2015). In this study, rainfall duration and initial slope gradient had significant influences on changes in slope gradient of the gully sidewalls (Fig. 9). When the rainfall intensity was constant, but the duration was increased, the dynamic and hydrostatic pressure caused by rainfall infiltration had an adverse effect on slope stability (Tu et al., 2009). In addition, the matric suction decreased or even disappeared with an increase in water content during rainfall infiltration, resulting in a decrease in soil shear strength, eventually leading to the occurrence of gravity erosion (Lomtadze et al., 1977; Tu et al., 2009). An increase in the initial slope gradient results in the concentration of shear stress at the sidewall toe and tension stress at the gully shoulder (Pei et al., 2013), leading to an increase in the absolute values of shearing forces, followed by slope failure. This indicates that mass failure led to a remarkable change in slope gradient during sidewall expansion. This result supports the finding of Claessens et al. (2013), which also proved that mass movement on the sidewall may be responsible for sudden and significant changes in the slope angle. In addition, the change in the slope gradient of the sidewall was negatively correlated with initial slope height in the experiments. The reason for this phenomenon may be that a higher slope height requires a greater amount of infiltration and more time for the rainfall to move from the top to the bottom of the soil profile on the gully sidewall.

Our results also indicate that the most significant factors affecting the retreat rate of the gully shoulder line were rainfall intensity and initial slope gradient (Fig. 10). The main reason for this is that runoff velocity rises with increasing slope gradient and rainfall intensity (Chen and Cai, 1990; Wang et al., 2013), which leads to the component of the tractive force of flowing water parallel to the slope surface to be greater than the soil resistance, eventually causing retreat of the gully shoulder line, leading to gully widening (Xiao and Tang, 2007). Demissie et al. (2019) also suggested that heavier and longer-lasting rainfall events had a substantial influence on channel width. As the initial slope gradient increases, the retreat rate of the gully shoulder line also increases. It is likely that the steep slope gradients encouraged the concentration of tension stresses at the top, which in turn led to the formation of tension cracks in the gentle slope near the gully shoulder line, and subsequent mass failure.

4.3 Hazards and defense scenarios

Gully sidewall expansion always causes land loss on the gentle slope. It is only when gullies threaten humankind that they represent a hazard (Ionita et al., 2015). The evolution of gullies has reduced the extent of agricultural land, which can diminish crop yields (Frankl et al., 2011; Zgłobicki et al., 2015). Before the ‘Grain-for-Green’ program in China, the Loess Plateau had been facing severe land loss due to sidewall expansion. For example, from 1958 to 1978, the average rate of sidewall retreat was 0.84 m a^{-1} in the Xingzi River Catchment in Yan'an City, and the annual loss of the inner-gully area was approximately 1886.7 hm^2 (Meng, 1996). Recently, several studies have shown that land loss on the gentle slope, caused by sidewall expansion, is still severe on the Loess Plateau. Li et al. (2015) found that, from 2003 to 2010, the maximum retreat rates of gullies in 30 investigated catchments in the southeastern part of the Loess Plateau ranged between 0.23 and 1.08 m a^{-1}, with an average of 0.51 m a^{-1}. It has been understood that, both before and after the 'Grain-for-Green' program in China, there was severe land loss on the gentle slope, caused by gully sidewall expansion. Qin et al. (2018) indicated that gully widening constituted approximately 80% of the total soil loss. Gully development caused by sidewall expansion is one of the greatest threats to land loss not only in China but also in other countries (Kuhnert et al. 2010). A field investigation in the Umbulo Catchment of southern Ethiopia indicated a rapid, downslope development of gullies in the past 30 years, with an average soil loss rate of between 11 and 30 t ha^{-1} a^{-1} (Moges and Holden, 2008). If gully sidewall expansion had not been controlled, gully expansion would have reached its maximum extent, forcing farmers to retreat, and reduce the cultivated area around the gullies (Yitbarek et al., 2012).

Only after the mechanisms of gully sidewall erosion have been understood, can effective measures be designed to reduce their expansion. Gully sidewall expansion results from the combined actions of water and gravity erosions. The importance of vegetation in controlling water erosion is widely accepted (Bochet et al., 2006). Vegetation plays a crucial role in intercepting rainfall and runoff, increasing infiltration capacity, stabilizing soil through root growth, protecting the soil surface against the direct impact of raindrops, and trapping sediment (Wei et al., 2009). In this study, the gully shoulders were eroded by rainfall and surface runoff, which promoted the occurrence and development of gravity erosion. Vegetation planted on gully shoulders could stabilize the gully and decrease runoff erosion (Nyssen et al., 2007). However, vegetation does not have a significant effect on controlling gravity erosion on the gully sidewall (Guo et al., 2019). With vegetation restoration on the Loess Plateau of China, the amount of soil erosion on the gentle slope has decreased, but the amount of soil erosion on the gully sidewall has become more prominent (Yang et al., 2011). The reasons are some unfavorable influences of vegetation on gully slope stability,

including the relatively high near-surface water content both during and after rainfall events (Simon and Collison, 2002). Our findings suggest that mass failure was the main cause of gully sidewall expansion, which is in agreement with the findings of Lohnes (1991) and Rowland et al. (2009). Consequently, treatment of the gravity erosion is the key to control gully sidewall expansion. Control measures for gully sidewall expansion cannot be effective, especially in the long term, if the gravity erosion is not considered to be the dominant mechanism in the gully sidewall expansion. For example, a structural practice implemented in the Yanwachuan Catchment of the Dongzhiyuan tableland on the Loess Plateau, involving simply filling the gully head with loess, was proved to be not effective (Wang et al., 2019). Simple gully landfill combined with drainage measures were also proved to be ineffective because the surface drainage on the downslope side always collapsed, triggered by washing and erosion. However, as a way to mitigate the risk of sidewall expansion, combining gully landfill and drainage with ecological slope protection can effectively control the mass failures (Wang et al., 2019). In addition, from a long-term perspective, the check dam has become an effective practice to control mass failure in gully areas on the Loess Plateau. The expansion of gully sidewall will be mitigated when the thalweg in the upper reach of the gully is increased and the height of the sidewall behind the check dam is reduced as a result of siltation behind the check dam (Xu et al., 2020). Thus, a combination of vegetation measures on the gentle slope, structural and ecological practices on the sidewall, and powerful structural practices, e.g., check dams, on the gully floor, is preferred for sidewalls vulnerable to expansion.

4.4 The way forward

In this study, rainfall and topographic factors were taken into account in an examination of gully sidewall expansion, although vegetation may influence and constrain such sidewall expansion. Although the Loess Plateau is characterized by low vegetation cover, the vegetation on the slope has recovered well in some areas through implementation of the 'Grain-for-Green' program. The roots of trees, shrubs, grasses and other plants play an important role in slope stability. Living plant roots can provide mechanical reinforcement to the soil (Chirico et al., 2013), which can resist the generation of tensile cracks, or can be converted into shear strength to resist shear stress. However, several studies have reported that vegetation can promote the initiation of mass movement on gully sidewalls during rainfall (Guo et al., 2019; Gao et al., 2020). For instance, Wang (2014) reported that sheet and rill erosion on the gentle slope was mitigated effectively through vegetation restoration, but that there was severe gravity erosion on gully sidewalls during a rainstorm in the Yanhe watershed on the Loess Plateau. Consequently, in future experiments, the effect of vegetation on gully sidewall expansion should be assessed.

New techniques can supplement traditional fieldwork that is based on visual observations and the use of erosion pins or stakes (Martínez-Casasnovas et al., 2004). On one hand, detailed studies and long-term monitoring activities on lateral gully expansion are neither frequent nor adequately documented in the existing literature, mainly because of the difficulties involved in investing human and economic resources on these phenomena, which are often considered a low hazard risk (Pasuto and Soldati, 2013). On the other hand, innovative monitoring techniques, such as the global positioning system (i.e., GPS) (Magri et al., 2008) and light detection and ranging (i.e., LiDAR) (Vianello et al., 2009), have already been used successfully in several studies dealing with ground deformation due to their high accuracy and reliability. Hence, to understand the kinematics, evaluate and mitigate the hazards, and predict evolutionary scenarios of gully sidewall expansion, there is a need to couple traditional monitoring with innovative monitoring techniques.

5 Conclusions

Land loss on the gentle slope was the result of the effect of water and gravity erosions, and gravity erosion was the primary cause. A strong positive correlation was found between the area of land loss on the gentle slope and the volume of gravity erosion (r_1 = 0.93), and the area of land loss on the gentle slope and the volume of water erosion also exhibited a positive correlation (r_2 = 0.71).

The gravity erosion is the major impetus of the change in slope gradient of the gully sidewall during the process of sidewall expansion in the experiments. As mentioned above, the amount of gravity erosion in 17 of the 19 rainfall events causing a change greater than 5° in the slope gradient of the gully sidewall accounted for more than 50% of the total amount of sidewall erosion. The retreat rate of the gully shoulder line showed a similar change with the total volume of sidewall erosion, exhibiting an increase-decrease-increase trend in the experiments. In addition, the retreat rate of the gully shoulder line was related to the volume of water erosion.

The rainfall duration and initial slope gradient had a significant influence on the change in slope gradient of the gully sidewall in the experiments. Meanwhile, the retreat rate of the gully shoulder line was highly susceptible to the rainfall intensity and initial slope gradient. The sensitivity coefficients of the change in slope gradient of the gully sidewall on the rainfall duration and initial slope gradient were 2.2 and 1.4, and the sensitivity coefficients of the retreat rate of the gully shoulder line on the rainfall intensity and initial slope gradient were 4.0 and 3.5, respectively.

Acknowledgments

This study was supported by the National Key R & D Project (2016YFC0402504), National Natural Science Foundation of China (No. 51879032), and Open Research Fund Program of Key Laboratory of Process and Control of Soil Loss on the Loess Plateau (201903).

References

Ali, A., Huang, J., Lyamin, A. V., Sloan, S. W., Cassidy, M. J. (2014). Boundary effects of rainfall induced landslides. Computers and Geotechnics, 61, 341–354.

Assouline, S., Ben-Hur, M. (2006). Effects of rainfall intensity and slope gradient on the dynamics of interrill erosion during soil surface sealing. Catena, 66, 211–220.

Blong, R. J., Graham, O. P., Veness, J. A. (1982). The role of sidewall processes in gully development; some NSW examples. Earth Surface Processes & Landforms, 7, 381–385.

Bochet, E., Poesen, J., & Rubio J. L. (2006). Runoff and soil loss under individual plants of a semi-arid Mediterranean shrubland: influence of plant morphology and rainfall intensity. Earth Surface Processes & Landforms, 31, 536–549.

Chaplot, V., Brown, J., Dlamini, P., Eustice, T., Janeau, J. L., Jewitt, G., Lorentz, S., Martin, L., Nontokozo-Mchunu, C., Oakes, E., Podwojewski, P., Revil, D., Rumpel, C., & Zondi, N. (2011). Rainfall simulation to identify the storm-scale mechanisms of gully bank retreat. Agricultural Water Management, 98, 1704–1710.

Chen, H., Cai, Q. G. (2006). Impact of hillslope vegetation restoration on gully erosion induced sediment yield. Science in China, Series D – Earth Sciences, 49, 176–192.

Chirico, G. B., Borga, M., Tarolli, P., Rigon, R., Preti, F. (2013). Role of vegetation on slope stability under transient unsaturated conditions. Procedia Environmental Sciences, 19, 932–941.

Chorley R. J. (1964). Geography and analog theory. Annals of the Association of American Geographers, 54(1): 127-137.

Claessens, L., Temme, A. J. A. M., Schoorl, J. M. (2013). Mass-movement causes: changes in slope angle. In J. Shroder (Ed. in Chief), R. A. Marston, & M. Stoffel (Eds.), Treatise on Geomorphology, vol. 7, Mountain and hillslope geomorphology. Academic Press, San Diego, pp. 212–216.

Demissie, B., Eetvelde, V. V., Frankl, A., Billi, P., Asfaha, T. G., Haile, M., Nyssen, J. (2020). Dynamics of ephemeral streams at the foot of degraded catchments in northern Ethiopia. Land Degradation & Development, 31, 591–606.

Frankl, A., Nyssen, J., Dapper, M. D., Haile, M., Billi, P., Munro, R. N., Deckers, J., Poesen, J. (2011). Linking long-term gully and river channel dynamics to environmental change using repeat photography (Northern Ethiopia). Geomorphology, 129, 238–251.

Gao, H., Xu, X. Z., Zhang, H. W., Jiang, Y. Z., Zhao, T. Q. (2020). How effective is vegetation in reducing gravity erosion on loess gully sidewall under intense rainfalls? Land Degradation & Development, 23, 157–166.

Guo, W. Z., Chen, Z. X., Wang, W. L., Gao, W. W., Zhao, M. (2019). Telling a different story: the promote role of vegetation in the initiation of shallow landslides during rainfall on the Chinese Loess Plateau. Geomorphology, 350, 106879.

Ionita, I., Fullen, M. A., Zgłobicki, W., Poesen, J. J. N. (2015). Gully erosion as a natural and human-induced hazard. Natural Hazards, 79, 1–5.

Jiao, J. Y., Wang, W. Z. (2001). Non-uniformity of the spatial distribution of rainfall on the Loess Plateau. Hydrology, 21, 20–24. (in Chinese).

Kuhnert, P. M., Henderson, A. K., Bartley, R., Herr, A. J. E. (2010). Incorporating uncertainty in gully erosion calculations using the random forests modelling approach. Environmetrics, 21, 493–509.

Li, Z., Zhang, Y., Zhu, Q. K., He, Y. M., & Yao, W. J. (2015). Assessment of bank gully development and vegetation coverage on the Chinese Loess Plateau. Geomorphology, 228, 462–469.

Liu Q., Wang Y., Zhang J. (2013). Filling Gullies to Create Farmland on the Loess Plateau. Environmental Science & Technology, 47(14): 7589-7590.

Liu, B. Z., Wu, F. Q. (1993). Gully erosion and its development on the loess plateau. Journal of the Northwest Forestry University, 8, 7–15. (in Chinese)

Liu, H., Deng, Q. C., Zhang, B., Li, X., Wang, L., Luo, M. X., Qin, F. C. (2016). Influences of different surveying and mapping methods on fractal characteristics of gully-head shoulder lines. Physical Geography, 37, 1–22.

Lohnes, R. A. (1991). A method for estimating land loess associated with stream channel degradation. Engineering Geology, 31, 115–130.

Lomtadze, V. D. (1977). Regularities of development of gravitational processes and their prediction. Bulletin of Engineering Geology and the Environment, 15, 9–12.

Lu, N., Godt, J. W. (2013). Hillslope Hydrology and Stability. Cambridge University Press, Cambridge, UK.
Magri, O., Mantovani, M., Pasuto, A., Soldati, M. (2008). Geomorphological investigation and monitoring of lateral spreading along the north-west coast of Malta. Geografia Fisica e Dinamica Quaternaria, 31, 171–180.
Martínez-Casasnovas, J. A., Ramos, M. C., Poesen, J. (2004). Assessment of sidewall erosion in large gullies using multi-temporal DEMs and logistic regression analysis. Geomorphology, 58, 305–321.
Meng, Q. M. (Ed.). (1996). Soil and Water Conservation on the Loess Plateau. Water Resources Press of the Yellow River, Zhengzhou, China, pp. 166–167. (in Chinese)
Moges, A., Holden, N. M. (2008). Estimating the rate and consequences of gully development, a case study of the Umbulo catchment in Southern Ethiopia. Land Degradation & Development, 19, 574–586.
Nyssen, J., Descheemaeker, K., Haregeweyn, N., Haile, M., Deckers, J., Poesen, J. (Eds.). (2007). Lessons learnt from 10 years research on soil erosion and soil and water conservation in Tigray. Tigray Livelihood Papers No. 7, Mekelle Zala-Daget Project, Mekelle University, K. U. Leuven, Relief Society of Tigray, Africa museum and Tigray Bureau of Agriculture and Rural Development, pp. 50.
Orense, R. P. (2011). Slope failures triggered by heavy rainfall. Philippine Engineering Journal. 25, 73–90.
Pasuto, A., Soldati, M. (2013). Lateral Spreading. In J. Shroder (Ed. in Chief), R. A. Marston, M. Stoffel (Eds.), Treatise on Geomorphology, vol. 7, Mountain and hillslope geomorphology. Academic Press, San Diego, pp. 239–248.
Pei, Q. T., Li, H. B., Liu, Y. Q., Jiang, J. G. (2013). Influence of slope gradient on distribution rule of geostress field in river valleys. Applied Mechanics and Materials, 404, 365–370.
Qin, C., Zheng, F. L., Wells, R., Xu, X., Wang, B., Zhong, K. (2018). A laboratory study of channel sidewall expansion in upland concentrated flows. Soil & Tillage Research, 178, 22–31.
Qin, W., Zhu, Q. K., Zhao, L. L., Qi, G. M. (2010). Topographic characteristics of ephemeral gully erosion in loess hilly and gully region based on RS and GIS. Transactions of the CSAE, 26, 58–64. (in Chinese).
Rowland, J. C., Dietrich, W. E., Day, G., Parker, G. (2009). Formation and maintenance of single-thread tie channels entering floodplain lakes: Observations from three diverse river systems. Journal of Geophysical Research, 114, F02013.
Sánchez-Canales, M., López-Benito, A., Acuña, V., Ziv, G., Hamel, P., Chaplin-Krame, R., & Elorza, F. J. (2015). Sensitivity analysis of a sediment dynamics model applied in a Mediterranean river basin: global change and management implications. Science of the Total Environment, 502, 602–610.
Simon, A., Collison, A. J. C. (2010). Quantifying the mechanical and hydrologic effects of riparian vegetation on streambank stability. Earth Surface Processes and Landforms, 27, 527–546.
Spalevic, V., Nyssen, J., Curovic, M., Lenaerts, T., Kerckhof, A., Annys, K. Van Den Branden, J., Frankl, A. (2013). The impact of land use on soil erosion in the river basin Boljanska Rijeka in Montenegro. Proceedings Agrosym 2013, Keynote Papers, pp. 54–63.
Tang, G. A., Zhao, M. D., Li, T. W., Liu, Y. M., Xie, Y. L. (2003). Modelling slope uncertainty derived from DEMs in loess plateau. Acta Geographica Sinica, 58, 824–830. (in Chinese).
Thornes, J. B., Alcantara-Ayala, I. (1998). Modeling mass failure in a Mediterranean mountain environment: climatic, geological, topographical and erosional controls. Geomorphology, 24, 87–100.
Tu, X. B., Kwong, A. K. L., Dai, F. C., Tham, L. G., Min, H. (2009). Field monitoring of rainfall infiltration in a loess slope and analysis of failure mechanism of rainfall-induced landslides. Engineering Geology, 105, 134–150.
Veness, J. A. (1980). The role of fluting in gully extension. Journal of Soil Conservation Service of New South Wales, 36, 100–108.
Vianello, A., Cavalli, M., Tarolli, P. (2009). Lidar-derived slopes for headwater channel network analysis. Catena, 76, 97–106.
Wang, C., Tang, G. A., Zhang, T., Li, Z. B., Wang, L., Wu, L. C. (2005). The study with high precision and high resolution of spatial variation of slope at small loess watershed with the erosion of rainfall. Journal of Mountain Research, 23, 589–595. (in Chinese).
Wang, L. Q., Liang, T., Zhang, Q. (2013). Laboratory experiments of phosphorus loss with surface runoff during simulated rainfall. Environmental Earth Sciences, 70, 2839–2846.
Wang, W. Z., Jiao, J. Y. (1996). Statistic analysis of the variation of rainfall and runoff-sediment yield process on slope surface in Loess Plateau Region. Bulletin of Soil and Water Conservation, 5, 21–28. (in Chinese)
Wang, X. F., Huo, A. D., Zhu, X. H., Zhao, Y. B., Jiang, C., Zheng, X. L. (2019). Study on governance mode of gully consolidation and highland protection project in East Gansu. Yellow River, 41, 106–109. (in Chinese).
Wang, Z. J. (2014). Characteristics of Vegetation and Erosion Sediment Yield in the Yanhe Watershed. Yangling: Research Center for Soil and Water Conservation and Ecological Environment, Chinese Academy of Sciences and Ministry of Education. (in Chinese)

Wang, Z. J., Jiao, J. Y., Rayburg, S., Wang, Q. L., Su, Y. (2016). Soil erosion resistance of Grain for green vegetation types under extreme rainfall conditions on the Loess Plateau, China. Catena, 141, 109–116.
Wei, W., Chen, L. D., Fu, B. J., Lv, Y. H., Gong, J. (2010). Responses of water erosion to rainfall extremes and vegetation types in a loess semiarid hilly area, NW China. Hydrological Processes, 23, 1780–1791.
Wijdenes, D. J. O., Bryan, R. B. (2010). Gully-head erosion processes on a semi-arid valley floor in Kenya: a case study into temporal variation and sediment budgeting. Earth Surface Processes & Landforms, 26, 911–933.
Wu, Y. Q., Zheng, Q. H., Zhang, Y. G., Liu, B. Y., Chen, H., & Wang, Y. Z. (2008). Development of gullies and sediment production in the black soil region of northeastern China. Geomorphology, 101, 683–691.
Xiao, C. C., Tang, G. A. (2007). Classification of valley shoulder line in loess relief. Arid Land Geography, 30, 646–653. (in Chinese).
Xu, X. Z., Liu, Z. Y., Xiao, P. Q., Guo, W. Z., Zhang, H. W., Zhao, C., Yan Q. (2015a). Gravity erosion on the steep loess slope: Behavior, trigger and sensitivity. Catena, 135, 231–239.
Xu, X. Z., Ma, Y. L., Yang, W. J., Zhang, H. W., Tarolli, P., Jiang, Y. Z., Yan, Q. (2020). Qualifying mass failures on loess gully sidewalls using laboratory experimentation. Catena, 187, 104252.
Xu, X. Z., Zhang, H. W., Wang, W. L., Zhao, C., Yan, Q. (2015b). Quantitative monitoring of gravity erosion using a novel 3D surface measuring technique: Validation and case study. Natural Hazards, 75, 1927–1939.
Xu, X. Z., Zhang, H. W., Zhang O. Y. (2004). Development of check-dam systems in gullies on the Loess Plateau, China. Environmental Science & Policy, 7, 79–86.
Yan, S. J., Tang, G. A., Li, F. Y., Zhang, L. (2014). Snake model for the extraction of loess shoulder-line from DEMs. Journal of Mountain Science, 11, 1552–1559.
Yang, J. S., Yao, W. Y., Ma, X. P., Shao, H., Wang, L. L. (2011). Progress of the gravity erosion and sediment yield study in the Loess Plateau. Yellow River, 33, 77–79. (in Chinese).
Yitbarek, T. W., Belliethathan, S., Stringer, L. C. (2012). The onsite cost of gully erosion and cost-benefit of gully rehabilitation: A case study in Ethiopia. Land Degradation & Development, 23, 157–166.
Zgłobicki, W., Baran-Zgłobicka, B., Gawrysiak, L., Telecka, M. (2015). The impact of permanent gullies on present-day land use and agriculture in loess areas (E. Poland). Catena, 126, 28–36.
Zhang, L., Tang, G. A., Li, F. Y., Xiong, L. Y. (2012). A review on research of loess shoulder-line. Geography and Geo-Information Science, 28, 44–48. (in Chinese)
Zheng, F. L., Xiao, P. Q. (2010). Gully erosion and sediment yield on the Loess Plateau. Beijing Science Press, 7 pp. (in Chinese)